Development of Scintillation Counters for the MINERνA Neutrino Detector

A thesis submitted in partial fulfillment of the requirement
for the degree of Bachelors of Science in Physics from
The College of William and Mary in Virginia.

by

Brian Andrew Wolthuis

Advisor: Dr. Jeffrey Nelson

Williamsburg, VA
May 2007

Abstract:

MINERνA (Main Injector ExpeRiment for ν-A) is a high statistics neutrino scattering experiment that has been approved to operate in the Neutrino Main Injector (NuMI) beamline at Fermi National Accelerator Laboratory. The goal is to build a detector to improve the interpretation of the data collected by the MINOS (Main Injector Neutrino Oscillation Search) experiment, which is currently in progress to study the phenomena of neutrino oscillations. The detector will be made up of planes of scintillator strips and is currently in the prototyping phase. Methods for improving overall plane uniformity and fiber polishing techniques were developed, and a radioactive source-based quality assurance test is currently being developed. Using a 10μCi ^{90}Sr beta source, a signal from a functional fiber within a plane was found to be on the order of 100Hz with no significant attenuation affects along the fiber. If the source is moved transversely from the fiber, there is a rapid fall-off in the signal strength. A stronger source will be necessary for a full-scale quality assurance testing for finished planes before they are incorporated into the MINERνA detector.

Acknowledgements:

I would first like to thank my advisor, Dr. Jeff Nelson, for taking a chance and giving me the opportunity to work on MINER*ν*A. It has been an honor to be part of such a significant and large scale scientific research project. A special thanks to Dan Damiani for working with me every day and explaining innumerable concepts and techniques over the last year. I would also like to thank Rita Schneider for taking all of my suggestions into consideration and making even the most mundane of tasks a pleasant experience. Both Dan and Rita were always willing to go to great lengths to help make my work a success in any way they could. Finally I would like to thank Meghan Snyder for igniting my interest in the project and for all of her late night explanations along the way.

Contents:

1. Introduction **5**

2. Detector and Technology Overview **6**

2.1. MINERυA Scintillator Design……..6

2.2. Detector Readout..…….7

2.3. Support and Fiber Routing……8

2.4. Flatness Testing…….8

3. Optics **11**

3.1. Optical Epoxy……...11

3.2. Optical Connectors……...13

4. **Assembly Testing** **14**

4.1. Optical Connectors……...14

4.2. Background Activity…….16

4.3. Source Based Quality Assurance……..17

4.3.1. Range of Signals……19

4.3.2. Count Rate vs. Source Position……..……...20

4.3.3. Fiber Attenuation……...22

5. Conclusions **23**

6. References **25**

1. Introduction

MINER*ν*A (Main Injector ExpeRiment for *ν*-A) is a high statistics neutrino scattering experiment that has been approved to operate in the NuMI (Neutrino Main Injector) neutrino beamline at Fermi National Accelerator laboratory. A fine-grained hexagonal detector made up of an array of scintillator strips will be used to detect interactions in the beamline. The goal of the detector is to improve the interpretation of the data collected by the MINOS (Main Injector Neutrino Oscillation Search) experiment, which is currently in progress to study the phenomena of neutrino oscillations.

Results from MINER*ν*A will reduce errors in the measured mass splitting measurements. The MINER*ν*A detector is to be placed directly in front of the MINOS Near Detector in MINOS Hall at Fermilab and will expand our knowledge of low energy neutrino interactions in the 1-18 GeV energy range. Figure 1 shows the planned detector in MINOS Hall.

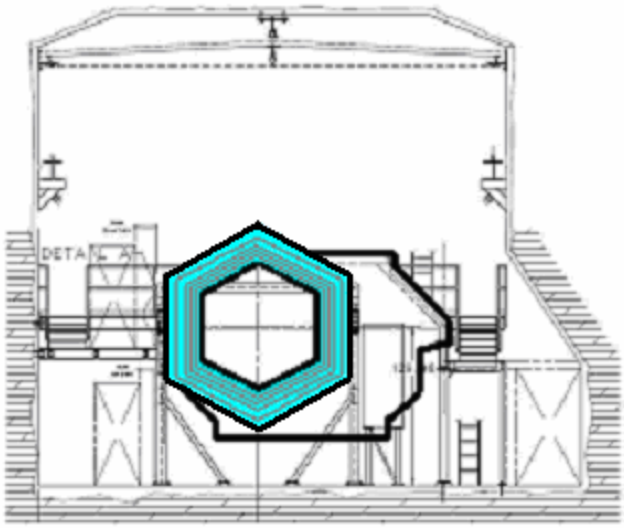

Figure 1: Schematic diagram of the MINERvA detector in front of the Near Detector in MINOS hall. The smaller hexagon is the MINERvA detector (OD in blue) and the irregular octagon (behind) is the MINOS Near Detector.

The two goals for this year's research were to develop and improve assembly techniques and to determine a procedure for testing the finished assemblies. Improvements in assembly

techniques are described later in this paper along with the current status of a quality assurance test for finished planes.

2. Detector and Technology Overview

2.1 MINERvA Scintillator Design

The MINER*v*A detector will consist of two main parts: an outer detector (OD) and an inner detector (ID). The outer detector is made up of six trapezoidal towers of scintillator and steel acting as a sampling calorimeter (Figure 2a). These trapezoids fit around the six edges of the hexagonally shaped inner detector. The inner detector is made up of 196 planes of scintillator arrays (Figure 2b). The array is a series of 127 scintillator strips cut at varying lengths and arranged to form a hexagon.

The cross section of an inner detector strip is a right isosceles triangle with a base of 3.3cm and height 1.7cm. The scintillator strips are made of polystyrene doped with organic molecules allowing for the detection of particle interactions via scintillation. Through each strip is a green wavelength shifting (WLS) fiber used to collect the scintillator light. Fibers are routed into groups of eight so that they may be glued into optical connectors and a signal reaching the fiber may be passed into a photomultiplier tube (PMT). The array is held in place by light tight sheets of black Lexan polycarbonate on the top and bottom. There is also a Lexan sheet of webbing throughout the plane (Figure 2c). The Lexan functions as structural support and also keeps stray light from the surroundings from reaching the scintillator.

Three prototype inner detector planes have been built to date. The first, Plane 0, was completed in Fall 2006 and sent to Fermilab as a structural and handling test. Much of the plane was destroyed during structural testing and mechanical autopsy by collaborators, but a large portion of the plane remained intact and was sent back to William & Mary for optical testing as

described in section 4.4. The other prototyping planes, Plane 1 and Plane 2, were completed in late Fall 2006 and early 2007, respectively. These two planes were sent to Fermilab as the first fully instrumented planes.

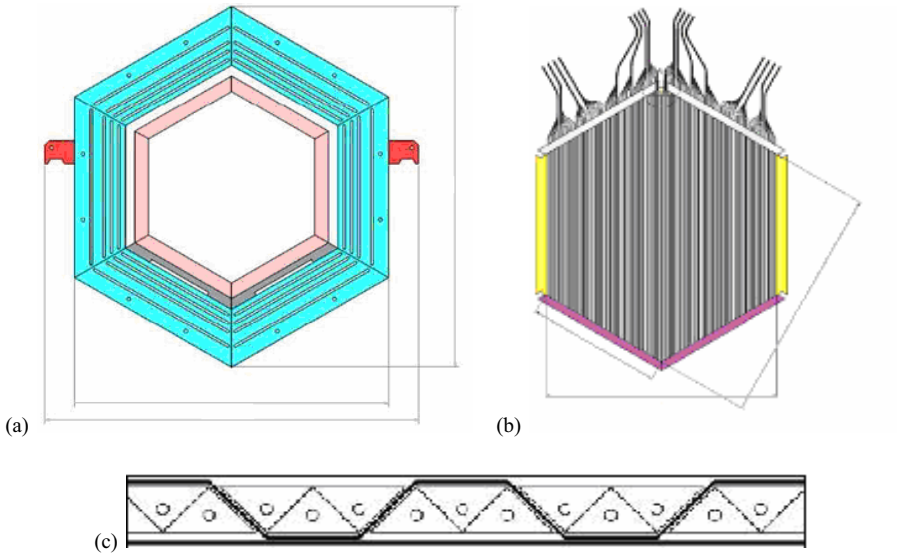

Figure 2: (a) Schematic diagram of the MINERvA outer detector with six towers of steel and scintillator. (b) Schematic diagram of inner detector with WLS fibers shown exiting the plane and routed into groups of eight. (c) Schematic cross-section of part of an inner detector scintillator array in a plane. The scintillator is shown as the triangles with Lexan webbing as the heavy black line through the triangles. The outer Lexan skins are the lines above and below the plane.

2.2 Detector Readout

As a charged particle travels through a plane, it excites electrons in the doped polystyrene of the scintillator. The electrons then drop back to a ground state and release energy in the form of ultraviolet photons. The light gets absorbed in a WLS fiber passing through the scintillator and re-emitted as green light. This change in wavelength is the result of a Stokes shift. The light then travels down the fiber until it reaches a photomultiplier tube (PMT), which turns the light signal into an electric signal with a gain of 10^6. This electric signal is amplified and measured as a voltage.

2.3 Support and Fiber Routing

Around the array of scintillator are six pieces of foamed PVC to hold the strips in place and provide support. On one side of the plane (two edges of the hexagon) the PVC is grooved to provide access to the fiber holes in the scintillator for epoxy injection (Figure 3a). On the opposite side, where the fibers exit the plane, the PVC is grooved to provide a routing for the fibers to the PMTs (Figure 3b). The side where the fibers exit the scintillator is called the detector readout end of the plane.

(a)  (b) 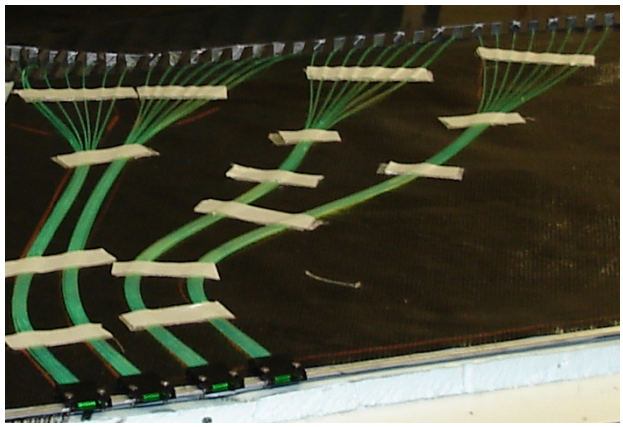

Figure 3: (a) Foamed PVC with grooves to supply access to the fiber holes. (b) The fibers are routed from the scintillator to the optical connectors in groups of eight.

2.4 Flatness Testing

The plane needs to be as flat as possible for maximum density of the detector. A smaller, more compact detector leads to fewer cracks around the detector and a more complete energy measurement. The variations in flatness of the plane are required to be less than 0.8 mm, or approximately 0.03 inches, to meet specifications. Using a set of calipers and a rigid straight edge, the distance from the highest point on the plane to the surface of the Lexan was measured to quantify the depth variation in the scintillator assembly. The straight edge was laid across the plane, and the distance from the straight edge to the assembly surface was measured at various

points along the plane. Figure 4 shows a schematic of the locations across the surface of the plane where measurements were taken, and Figure 5 is a plot of the results.

The flatness measurements show that the depth variation in the surface of the plane was up to 0.16 inches. Although the flatness of Plane 1 was an improvement over Plane 0, it was not satisfactory for use in the detector. The plane appeared highest along strip 51 and lowest along strip 72.

Qualitatively, the flatness of each plane continues to improve due to advances in construction techniques. A system of pins and fixtures was developed and used on Plane 2 to improve the uniformity of the plane. The system includes fixing the PVC pieces around the plane to the workstation table with pins and using a set of plastic pieces to evenly space the strips within the plane. After the PVC pieces have been fixed to the table, half of the scintillator strips are laid out in their positions on the bottom skin of Lexan. These are the strips that are underneath the Lexan webbing in the plane. Plastic combs that have been cut to the appropriate dimensions are then used to evenly space the strips. The spacing is also positioned by two plastic pieces that temporarily replace the PVC at one end of the plane and have pins protruding along the inner edge that fit into the ends of the scintillator strips. These two pieces along with the plastic combs force the proper alignment of the strips under the Lexan webbing. This stage of the construction is shown in Figure 6. After the bottom strips are properly aligned, the Lexan webbing is attached, and the rest of the strips are put in place and aligned again using the two plastic pieces with protruding pins. Finally, the top Lexan skin is glued onto the surface and the PVC pieces around the edges are fastened to the plane.

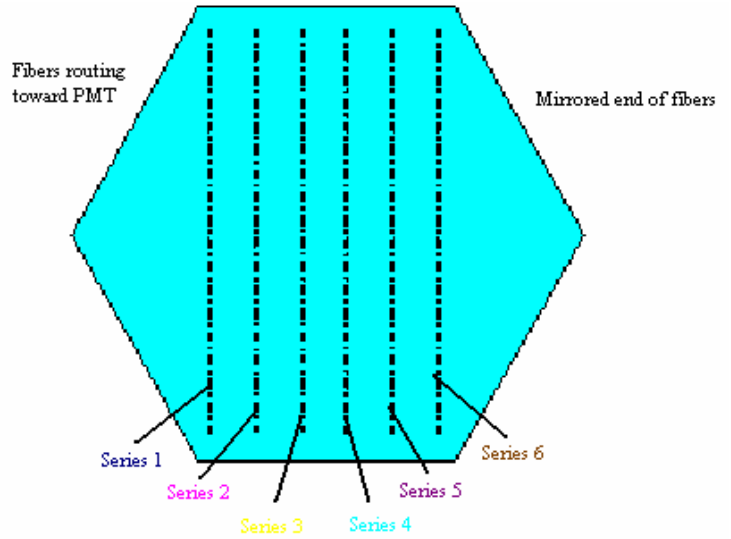

Figure 4: Surface of plane showing locations of depth measurements. Each line of measurements is related to a series in the graph below.

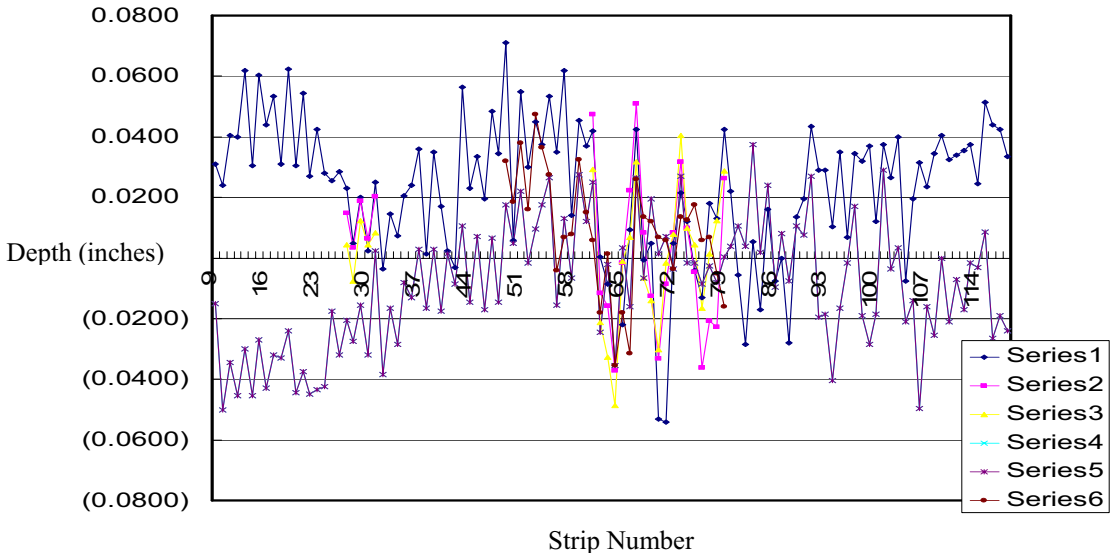

Figure 5: Flatness measurements (in inches) vs. strip number normalized to central region of the plane. Each series is related to a line in the figure above.

The delivery schedule of Plane 2 did not allow for quantitative depth variation measurements. Simple tests showed that the flatness of Plane 2 had variations of about 0.05 inches, but the measuring technique was not rigorous.

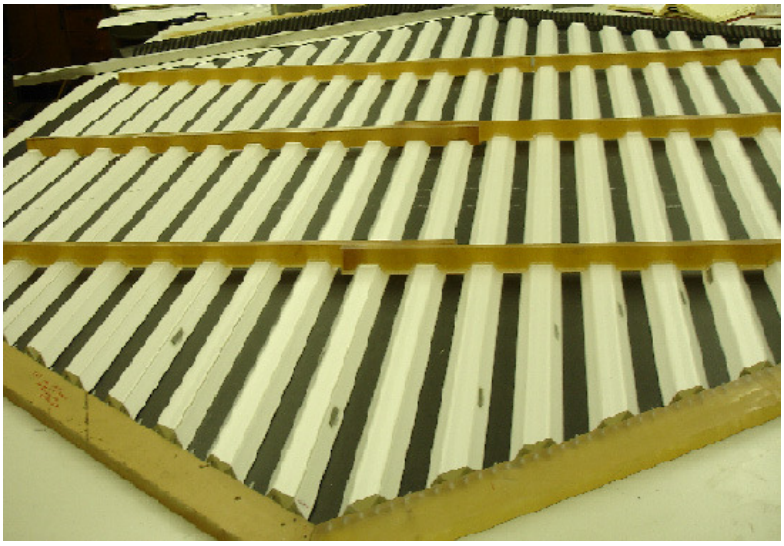

Figure 6: A picture of a plane being constructed using the new pins and fixture system. Half of the strips have been laid out and are ready for the Lexan webbing to be added. The strips are held in place around the edges by PVC fixed to the table and a series of combs keep the strips properly spaced.

Also to further improve flatness and uniformity for future planes, a system of aluminum structures has been constructed to support the workstation and new laminated tabletops that have been ordered. Using these new surfaces, a plank method of plane construction will be tested this summer. The plank method will consist of building smaller sections of the plane and splicing the sections together rather than constructing the entire plane at once.

3. Optics

3.1 Optical Epoxy

Inside the fiber holes, there is a cushion of air between the fibers and the scintillator. This has an effect on how much light from the excited electrons actually makes it into the WLS fiber. Any time light is passing out of one medium into another, reflection occurs at the interface. The index of refraction of each material determines how much reflection and

transmission occurs. The index of refraction (n) is 1.5 for scintillator, 1 for air, 1.4 for the fiber coating, and 1.55 for the fiber core itself. Applying the equation

$$t = 1 - \frac{n_2 - n_1}{n_2 + n_1}$$

at each interface, where t is the transmission coefficient and n is the index of refraction for each medium, the theoretical transmission yield of light traveling from the scintillator into the fiber is 63.3% for normal incidence. If the light hits the fiber hole with an angle of incidence other than zero, total internal reflection causes the average transmission to drop further. This is dramatically improved by filling the air in the fiber holes using a medium with an index of refraction much closer to that of the scintillator and fiber coating than the index of refraction of air. The substance used is an optical epoxy with an index of refraction of 1.45. Using the same calculations for normal incidence but replacing air with epoxy, the theoretical yield becomes 91.6%. Again, at varying angles of incidence, total internal reflection reduces the theoretical yield.

The materials employed were tested by Meghan Snyder, but the epoxy injection techniques she employed were not sufficient for the full scintillator strip length used in the planes. The epoxy used is a mixture of 100:14 by mass Epon 815C resin to Epi-Cure 3234 (TETA) hardener. After the epoxy is mixed, it is poured into a syringe. The pressure needed to expel the epoxy from the syringe comes from an air driven glue machine that hooks up to the back of the syringe. The needle at the end of the syringe is poked through a small PCV wedge coated with petroleum jelly and two gaskets to serve as a stopper for backflow. The end of the needle is put into the fiber hole so that the gasket is flush against the surface of the scintillator around the hole. The epoxy is injected down the fiber hole until it has filled the void around the fiber. A picture of the syringe is shown in Figure 7.

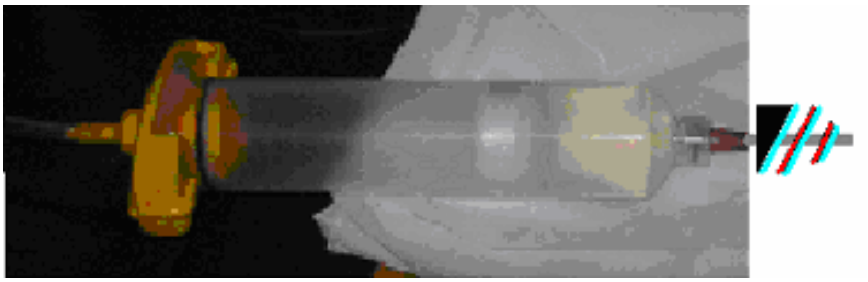

Figure 7: An epoxy-filled syringe with needle through a schematic of PVC wedge (black), Vaseline (blue), and gaskets (red).

Originally, a silicone sealant had been used in place of the wedge and gaskets. This sealant was ineffective because back pressure popped it off during injection into the longer strips, causing backflow and an uneven distribution of epoxy within the hole. The wedge and gasket technique was developed as an effective solution to the problem and has now been adopted as part of the production technique.

3.2 Optical Connectors

The fiber routing leads the fibers from the scintillator to the PMT. The fibers are gathered in groups of eight and fed into an optical connector box. The connector box, which serves as a connection between fibers coming from the plane and the fibers going into a PMT, consists of three parts. First is the ferrule that holds the fibers. The fibers are glued into the ferrule using the same mixing and injection methods as those used for filling the fiber holes in the scintillator strips with optical epoxy. The ferrules are then snapped into a spring-loaded clip. Figure 8 shows the ferrule and clip pieces before and after being put together with the fibers. The ferrule and clip with fibers routed through are then polished using a diamond bit in a fly-cutter. The third part of the box is a DDK format connector box. Clips can be inserted into either end of the connector so that the fibers properly align themselves for maximum light transmission through the connectors.

(a) 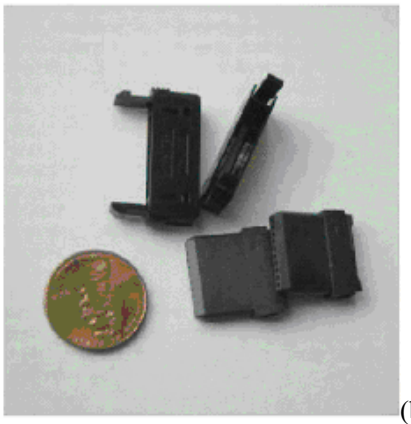 (b) 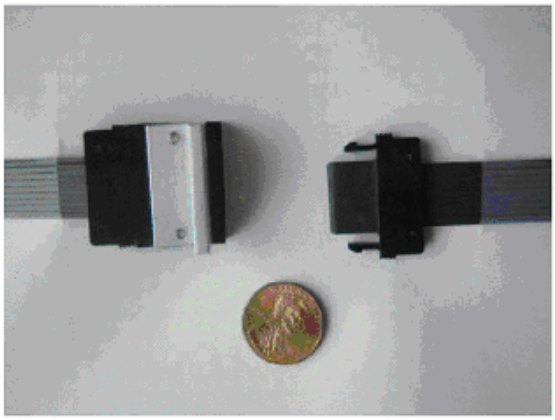

Figure 8: DDK connector Parts. (a) The top pieces are clips and the bottom pieces are ferrules. (b) The fibers have been glued into place along with the ferrules into the clips. The left clip is in the connector box and the right clip has been disconnected. When both clips are in the box, the fibers line up and make contact.

4. Assembly Testing

4.1 Optical Connectors

A series of tests led to the development of a polishing technique to ensure efficient transmission of light through the optical connectors. To test the technique, the transmission through a DDK connector box was measured on five cables, where one cable includes eight fibers coupled to a ferrule and clip on both ends. Five cables of clear fiber, labeled 23-27, were tested at Fermilab for transmission. These fibers were shipped to William & Mary where they were cut. The cut ends were glued into new ferrules and clips using the standard optical coupling procedure. The fibers were then polished using a fly-cutter with a diamond bit and an end mill so that the ferrules could be clipped back together using a DDK connector box. The cables were sent back to Fermilab for transmission testing through the connector. Figure 9 is a schematic showing the process of fiber cutting and reattachment through DDK connector.

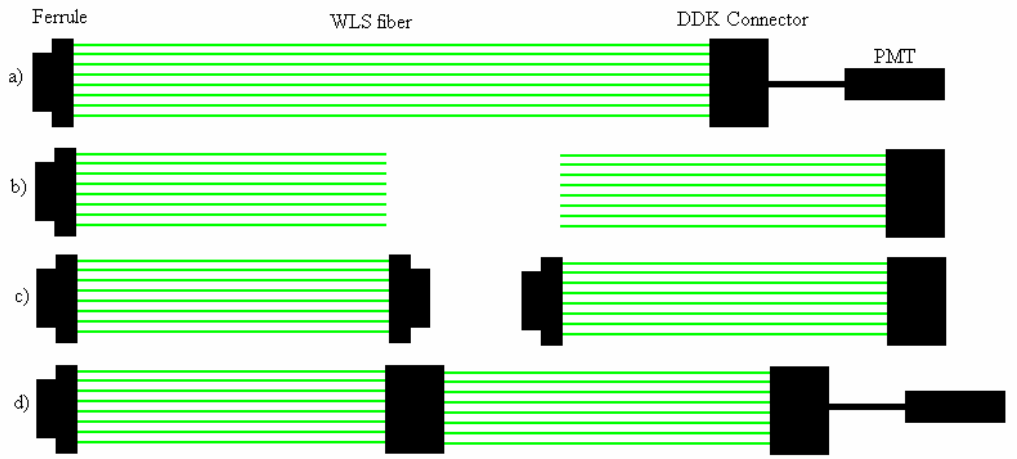

Figure 9: Schematic of the transmission testing process. a) An uncut cable is connected to a PMT for testing. b) The cable is cut across all eight fibers. c) The cut fibers are coupled with a connector pieces. d) The fibers are connected and retested.

	Cable 23	Cable 24	Cable 25	Cable 26	Cable 27
Average	75.50%	79.70%	69.50%	82.00%	79.10%
Standard Deviation	2.00%	1.80%	5.50%	2.90%	1.50%

Table 1: Raw transmission data of light through each connector after cutting.

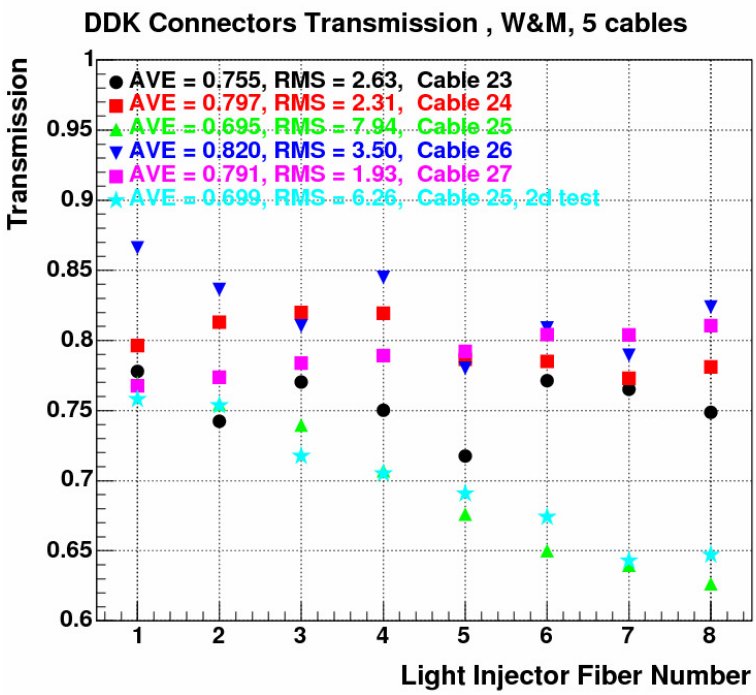

Figure 10: Plot of fraction of light transmitted through each fiber after cutting and calibration. (Calibration and graph by Howard Budd.)

The results show a consistent transmission through four of the connectors. Connector 25 shows an overall decrease in light yield. Examination showed a black smudge on the end of the fibers in that connector. The source of this material was never identified, and it has not been observed in subsequent tests. This smudge is the most likely cause for the decrease in transmission.

The required specification for light yield through a connector is 75%, and the results of this fiber polishing technique consistently meet this specification. The procedure was approved with the addition of a visual examination of the polished fiber.

4.2 Background Activity

Any light not coming from the particles passing through the plane degrades the signal and adds error to position measurements. This light could be a result of light leaks in the plane or radioactivity from the surrounding material. The background activity was measured using a single fiber to measure possible radioactivity of the materials being used in plane construction and to get a baseline value for background activity.

The materials tested included outer detector scintillator strips, Lexan, electrical tape in place of Lexan, Eljen paint over the end of the strip, Scotch-Weld DP-190 translucent epoxy to couple the Lexan to the strip, and Scotch-Weld DP-190 gray epoxy to couple the Lexan to the strip. One green WLS fiber was glued into an optical connector using the standard optical coupling procedure. This fiber was used to test background activity in seven combinations of materials to find any potential signal-degrading activity. The ferrule was connected to a PMT by a DDK connector and the light captured in the fiber was measured as a current using a picoammeter. Two sets of measurements were made for each combination to determine systematic errors. The setup of the equipment is shown schematically in Figure 11.

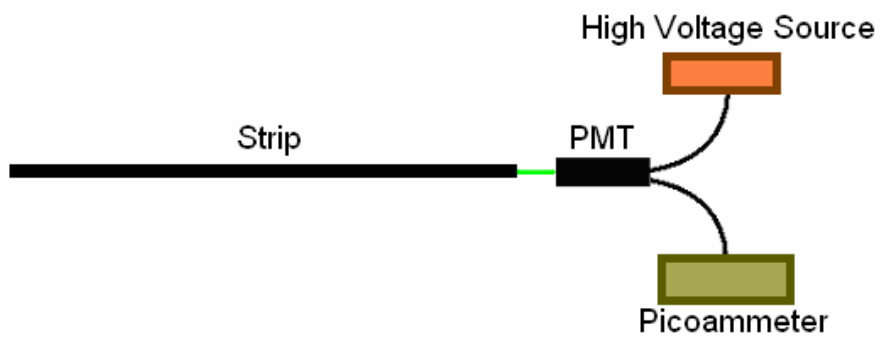

Figure 11: Schematic diagram of background testing apparatus with green WLS fiber inserted into a strip and connected to a PMT. The current is read out of a picoammeter.

Sample	Scintillator	Lexan	Electrical Tape	Eljen paint	Translucent epoxy	Gray epoxy	I1 (nA)	I2 (nA)
1							4.2	3.5
2		x					4.1	3.5
3	x		x				3.1	3.6
4	x	x					3.5	3.7
5	x	x		x			3.8	3.7
6	x	x			x		3.4	3.7
7	x	x				x	3.5	3.5

Table 2: Background activity using a fiber in different materials.

Sample 1 is the control sample with only the light-tightened fiber. The results show no evidence that any of the materials tested give enough radioactivity to degrade the signal above the level seen in sample 1. The readings were all between 3.1nA and 4.2nA, which falls in the same range as general background activity after light tightening. The lowest reading came from the strip wrapped in electrical tape, which is believed to be the most light-tight wrapping technique. The highest reading came from the bare fiber on the first reading, which is most likely due to a small light leak that was addressed before the second trial. Any variation in the current read by the ammeter was within the variation in the control sample. All the materials tested were found to be suitable for use in the MINERνA detector.

4.3 Source Based Quality Assurance

A source based quality assurance test needs to be designed to assess each plane for optical defects prior to shipping. The main concern is the condition of the fibers, which lose

their function if they are over-bent or broken. A light source is necessary because the plane assemblies are light-tight. A radioactive source allows light to be generated in the scintillator and be trapped in the fiber. This light will show up as a signal after passing through a PMT, and the signal will give confirmation that the fiber is intact and working.

A series of tests were run on what was left over of Plane 0 to gather data on what properties can be expected from an actual plane. The same fiber used to test background activity was used to determine the properties of a functional fiber in Plane 0. When exposed to the source, one end of the fiber was inserted into a scintillator strip and the other was connected to a PMT and picoammeter.

A radioactive source was used to stimulate the scintillator. The initial experiment used a 10μCi ^{137}Cs source, a gamma source that would penetrate deep into the plane, illuminating both top and bottom strips. This source, however, was not active enough to induce a significant signal. The hotter gamma sources available were not practical for use in this test due to the cumbersome 80 pound tungsten shielding required.

Instead, a beta source, ^{90}Sr, was available. Beta particles are quickly attenuated in the material, but those from ^{90}Sr have a high enough energy to be useful. Also, collimated beta sources tend to continue traveling in one direction beyond the collimator, where the gamma particles would spread out over a large number of strips due to Compton scattering.

Three tests were run with a collimated 10μCi ^{90}Sr beta source placed on the top surface of the plane above the fiber. The first test consisted of a series of measurements taken to find what kind of signal could be expected from a particle hitting the plane at various locations along the surface. The second test was a measurement of light output versus transverse source position

on a top and bottom strip of the plane. The third test was to determine the attenuation properties of the fiber.

The fiber was inserted into the strip to be tested and connected to the PMT using an optical connector, just as in the background activity tests. The signal from the PMT was then amplified by three 10x amplifiers and sent through a discriminator. The discriminator was set to cut out any signal below 1.5 photoelectrons to reduce noise from single photoelectron sources. Beta sources should give signals of many photoelectrons. The signal was then counted by a scaler, which was set to measure counts in 10 second periods. The test configuration is shown in Figure 12.

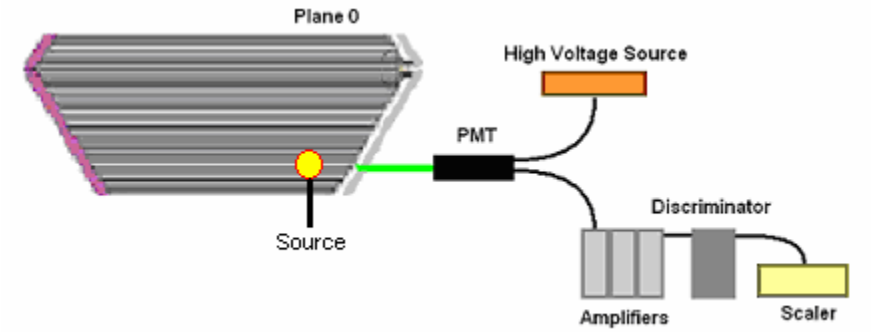

Figure 12: Schematic diagram of source tests with Plane 0 with green WLS fiber inserted into a strip and connected to a PMT. The PMT is connected to a series of 3 10x amplifiers, a discriminator, and the measurements are made using a scaler.

Each time data was recorded, five measurements were taken and averaged. Before each set of five measurements were made, the plane was light-tightened and a set of five background readings was taken. This assured that the background activity could be accurately subtracted from the data collected.

4.3.1 Range of Signals

In the first test, measurements were taken to get an idea of the number of signals that could be expected at different points along the surface of the plane. The goal was to find a dynamic range of values, so measurements were taken near the readout end of short strips as well

as long strips using the full length of the fiber. The fiber was inserted into strip 110, which was a short top strip near an edge of Plane 0. The source was placed 11cm from the readout end of the strip and readings were taken. Measurements were also taken at 54cm and 146cm of the same strip. The fiber was then removed from strip 110 and moved into strip 65, the longest top strip in the plane. The source was placed near the end of the fiber at approximately 190cm from the readout end of the strip and measurements were taken. Each of the measurements made in the top strips 110 and 65 were repeated in their adjacent bottom strips 109 and 64.

The readings showed a range from on the order of 100Hz above background down to near background levels. The highest reading, 104Hz, came from the short top strip where the source was close to the readout end of the strip. The higher values close to the readout end of the strips compared with the far end are most likely due to some attenuation in the fiber. As expected, the lowest readings came when using the bottom strip. These low rates indicate that a stronger source will be required to get statistically significant readings.

4.3.2 Count Rate vs. Source Position

To measure signal counts versus position, only one top strip and one bottom strip were used. The fiber was inserted into a top strip and the source was placed directly over the fiber in the center of the strip. The source was then moved transversely in 4mm increments up to 20mm in each direction perpendicular to the strip. The fiber was then moved to an adjacent bottom strip and each measurement was repeated.

The results for the top strip show that there is a rapid falloff as the source is moved from directly above the fiber. The strips are only 33mm wide, so when the source is no longer above the strip at +/- 17mm, the signal falls back to background levels. Apart from the reading at

Signal Counts vs. Source Position

Top Strip	Count Rate (Hz)										
Source Position (mm)	-20	-16	-12	-8	-4	0	4	8	12	16	20
Count Rate (Hz)	**-2**	**11**	**51**	**3**	**49**	**43**	**32**	**20**	**21**	**14**	**-1**
Error	2.16	2.23	2.32	2.33	2.33	2.30	2.29	2.30	2.23	2.23	2.21
Bottom Strip	Count Rate (Hz)										
Source Position (mm)	-20	-16	-12	-8	-4	0	4	8	12	16	20
Count Rate (Hz)	**6**	**0**	**8**	**2**	**8**	**12**	**2**	**-5**	**3**	**0**	**5**
Error	1.61	1.60	1.60	1.62	1.61	1.64	1.60	1.59	1.55	1.55	1.57

Table 3: Count rate above background of source above background resulting from changes in source position.

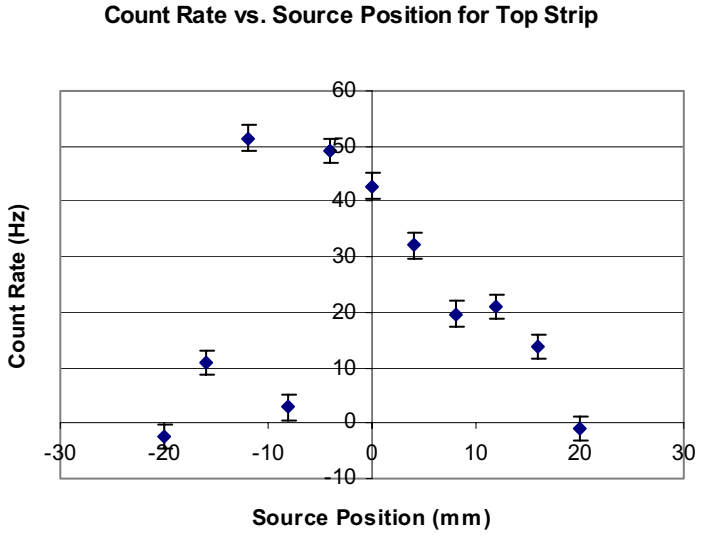

Figure 13: Count rate as a function of transverse position of the source using a top strip.

-8mm, the results are smoothly distributed, given that the 0mm mark may not be the exact center of the strip. The point at which the signal drops to background levels appears very close to the edges of the strip.

The center of the strip was found by locating the edges of the strip under the Lexan and approximating the middle, which is a possible source of error in these measurements. A better fixing technique will need to be developed to more accurately find the center of strips relative to their edges.

The results from the bottom strip with this source showed small signals and give little useful information. The only significant signal occurs very close to the center of the strip. The beta particles coming from the source do not allow penetration deep into the scintillator, so small count rates are expected. In the top strips, the data was still useful until the edge of the strip because the beta particles could still stimulate the electrons in the scintillator. In the bottom strips, a stronger source is needed to collect useful data to check light yields for quality assurance purposes.

4.3.3 Fiber Attenuation

In measuring the attenuation properties of the fiber, the fiber was placed in one of the longest top strips in the center of the plane, and measurements were taken with the source at 10cm increments along the length of the strip. The first measurement was 10cm from the readout end of the strip and the final was at 190cm, near the end of the fiber within the strip.

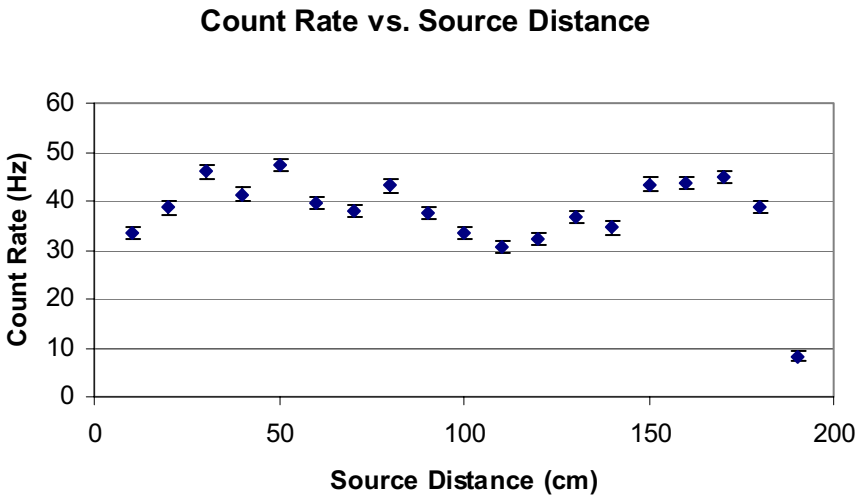

Figure 14: Count rates at varying distances along the length of a top strip.

The results show little attenuation along the fiber within the strip even at large distances. A possible source of error may be that the source was not directly above the fiber at each point. The only significant drop-off in signal occurs at 190cm, which is at the very end of the fiber.

5. **Conclusions**

The MINERvA detector is currently in the prototyping phase. Three inner detector planes have been completed during this project. Each successive plane provided an opportunity for improving construction techniques as well as assessment of the resulting assembly.

The flatness of Plane 1 was assessed quantitatively, and although there was significant improvement over the uniformity of Plane 0, Plane 1 was not satisfactory for use in the functional detector. A system of pins and fixtures was developed to enhance uniformity in future planes and was put to use during the building of Plane 2. The flatness was improved, and higher quality workspaces and a plank system for construction may allow for further improvement.

An effective polishing technique for the optical connectors in the detector was also developed and tested. Using a diamond bit in a fly-cutter to polish the fibers, the transmission through these connectors meets the specifications required for use in the detector.

Background activity was tested using the materials that are being used during plane construction. The results show no evidence of potential signal-degrading radioactivity in the selected materials.

Three tests were run on Plane 0 using a 10μCi ^{90}Sr beta source, as the available gamma sources were not practical for testing due to the heavy shielding required. First was a test to find a range of signal counts that can be expected by placing the source at various locations over the surface of the plane. The maximum values show a signal on the order of 100Hz while using a top strip. The second test displayed the effects of the transverse position of the source relative to the center of the strip. Clearly the signal is strongest when the source is over the fiber rather than toward the edges of the strip. In both of these tests, the lower values resulting from using a bottom strip suggest that a stronger source will be required for a useful source-based quality

assurance test. The third test using a source was determining the attenuation properties of the fiber. The results show little evidence of any significant attenuation along the fiber when using a ^{90}Sr source and a 1.5 photoelectron threshold.

The next step is to find a practical source that can be used to test future planes. The source must be strong enough to interact with both top and bottom strips to give useful information on the condition of the fibers. The source must be set up so that it can accurately test different locations over the surface of the plane. Finally, the procedure for a full-scale quality assurance test must be developed to ensure the functionality of the finished planes that will be used in the MINERνA detector.

6. **References:**

Jeff Nelson, College of William and Mary, private communication.

Dan Damiani, College of William and Mary, private communication.

Rita Schneider, College of William and Mary, private communication.

Meghan Snyder, "Design of the Scintillator Counters for the MINER*ν*A Neutrino Detector," Senior Thesis, College of William and Mary (2006). Private communication.

Kelly Sassin, College of William and Mary, private communication.

Robert Flight, University of Rochester, Mechanical engineer, private communication.

Dan Ruggiero, University of Rochester, Technician, private communication.

Howard Budd, University of Rochester. MINER*ν*A Document 1163-v3. "FMP plane construction update." http://minerva-docdb.fnal.gov:8080/. Private communication.

"Technical design report for MINER*ν*A detectors," The MINER*ν*A Collaboration, NUMI-L-703, (2006).